AIAA Journal
Vol. 48, No. 6, June 2010

Random Eigenvalue Problems in Structural Dynamics: Experimental Investigations

S. Adhikari*
Swansea University, Swansea, England SA2 8PP, United Kingdom
and
A. Srikantha Phani†
University of British Columbia, Vancouver V6T 1Z4, Canada

DOI: 10.2514/1.44668

This paper presents two experimental investigations of uncertainty in natural frequencies of linear structures estimated from measured frequency response function under dynamic loading. Experiments were conducted on 100 nominally identical realizations of two structures: a fixed–fixed beam and a thin plate with one edge fixed and the remaining three edges free. In the first set of experiments, on a fixed–fixed beam, 12 identical masses were placed at random spatial locations (generated by a computer) along the length of the beam. Each random arrangement of the masses constitutes one realization, and 100 such realizations were individually subjected to impulse loading to obtain frequency response functions. The total random mass is about 2% of the total mass of the beam. In the second set of experiments, 10 spring-mass oscillator units were attached to the cantilevered plate at random spatial locations determined from a computer-generated random matrix. Although the beam experiments represent parametric uncertainty in the mass matrix, the plate experiment pertain to unmodeled dynamics, which in turn results in randomness in both the mass and stiffness matrices. The results obtained from these experiments may be useful for the validation of many random eigenvalue analysis and prediction methods currently available to structural dynamicist. This paper is limited to comparisons with Monte Carlo simulation of deterministic finite elements models of the two structures. It is concluded that the method of estimation of natural frequencies from frequency response functions and the spatial location of the measurements has significant influence upon the first two moments (mean and standard deviation) of the natural frequency ensemble. Furthermore, although the Monte Carlo simulation estimates of the mean and standard deviation are in reasonable agreement with experiments at higher frequencies, the probability density function differ appreciably, within the limits of the sample size investigated in this study.

Nomenclature

$\mathbf{K}$ = stiffness matrix
$\mathbf{M}$ = mass matrix
N = degrees of freedom of the system
$p_{(\cdot)}$ = probability density function of $(\cdot)$
$\mathbb{R}$ = space of real numbers
$\delta(\cdot)$ = random part of $(\cdot)$
λ_j = eigenvalues of the system
$\boldsymbol{\phi} j$ = eigenvectors of the system
$\overline{(\cdot)}$ = nominal (deterministic) part of $(\cdot)$

I. Introduction

THE characterization of natural frequencies and mode shapes requires the solution of a linear eigenvalue problem in the analysis and design of engineering systems subjected to dynamic loads. This problem could either be a differential eigenvalue problem or a matrix eigenvalue problem, depending on whether a continuous model or a discrete model is envisaged. The description of real-life engineering structural systems is inevitably associated with some amount of uncertainty. Parametric uncertainty pertains to material and geometric properties, boundary conditions and applied loads. When we take account of these parametric uncertainties, it is imperative to solve *random eigenvalue problems* to obtain the dynamic response statistics, such as the mean and standard deviation of displacement and stress amplitudes. Random eigenvalue problems also arise in the stability analysis or critical buckling loads calculation of linear structural systems with random imperfections. Random eigenvalue problem arising due to parametric uncertainty can be efficiently formed using the stochastic finite element method (see, for example, [1–8]). The study of probabilistic characterization of the eigensolutions of random matrix and differential operators is now an important research topic in the field of stochastic structural mechanics. Boyce [9], Scheidt and Purkert [10], Ibrahim [11], Benaroya [12], Manohar and Ibrahim [13], and Manohar and Gupta [14] are useful sources of information on early work in this area of research that also provide a systematic account of different approaches to random eigenvalue problems.

The majority of the studies reported on random eigenvalue problems are based on analytical or simulation methods. Simulation-based methods are often used to validate approximate but relatively fast prediction tools (such as perturbation based methods). Experimental results are rare because of difficulties such as 1) the cost involved in generating nominally identical samples of a structural system, 2) the resources and effort involved in testing a large number of samples, 3) the repetitive nature of the experimental procedure, and 4) ensuring that different samples are tested in exactly the same way so that no uncertainty arises due to the measurement process. In spite of these difficulties some authors have conducted experimental investigations on random dynamical systems. Kompella and Bernhard [15] measured 57 structure-borne frequency response functions at driver microphones for different pickup trucks. Fahy [16] (page 275) reported measurements of FRFs on 41 nominally identical beer cans. Both of these experiments show variability in nominally identical engineered systems. Friswell et al. [17] reported two experiments in which random systems were created in the laboratory for the purpose of model validation. The first experiment used a randomly moving mass on a free–free beam and

Received 31 March 2009; revision received 5 September 2009; accepted for publication 7 September 2009.

*Chair of Aerospace Engineering, School of Engineering, Singleton Park; S.Adhikari@swansea.ac.uk. Senior Member AIAA.

†Assistant Professor, Department of Mechanical Engineering, 2054-6250 Applied Science Lane.

the second experiment comprised a copper pipe with uncertain internal pressure. Fifty nominally identical random samples were created and tested for both experiments.

In contrast with analytical studies, in the present experimental study, the eigenvalues are deduced from the measured frequency response functions using system identification techniques. Thus additional uncertainties may likely to be introduced by the method of system identification employed even if other uncertainties, within the control of the experimenter, were minimized. In a recent work, Shiryayev et al. [18] discussed the difficulties and uncertainties associated with the system identification methods in the context of a bolted joint model. To improve the reliability of the results, two system identification techniques are contrasted in this regard: rational fractional polynomial (RFP) method [19], and the nonlinear least-squares (NLS) technique [19]. Each system identification technique is applied to the two experimental test cases, described later. The difference between this data and previous experimental data is that the tests are closely controlled. This allows one to model uncertainty, propagate it through dynamical models and compare the results with experiments.

We begin with a brief introduction to random eigenvalue problems in Sec. II. The first experiment, described in Sec. III is on a fixed–fixed beam with 12 masses placed at random locations. The total amount of random masses is about 2% of the total mass of the beam. This experiment is aimed at simulating random errors in the mass matrix. The second experiment, described in Sec. IV, considers a cantilever plate with 10 randomly placed spring-mass oscillators. This experiment is aimed at simulating unmodeled dynamics, which in turn leads to randomness in the mass and stiffness matrices. For both experiments, 100 nominally identical dynamical systems are created and tested separately. The probabilistic characteristics of the frequency response function are discussed in the low-, medium-, and high-frequency ranges. The data presented here are available on the for research purposes.[‡] This data may be useful to validate different uncertainty quantification and propagation methods in structural dynamics.

II. Random Eigenvalue Problems

The random eigenvalue problem of undamped or proportionally damped discrete, or discretized continuous, systems can be expressed by

$$\mathbf{K}\boldsymbol{\phi}_j = \lambda_j \mathbf{M}\boldsymbol{\phi}_j \tag{1}$$

where λ_j and $\boldsymbol{\phi}_j$ are the eigenvalues (natural frequency squared) and the eigenvectors (mode shapes) of the dynamical system. It is assumed that $\mathbf{M}$ and $\mathbf{K}$ are symmetric and positive definite random matrices so that all the eigenvalues are real and positive. We consider randomness of the system matrices of the following form:

$$\mathbf{M} = \bar{\mathbf{M}} + \delta\mathbf{M} \quad \text{and} \quad \mathbf{K} = \bar{\mathbf{K}} + \delta\mathbf{K} \tag{2}$$

Here, $\overline{(\cdot)}$ and $\delta(\cdot)$ denote the nominal (deterministic) and random parts of $(\cdot)$, respectively. Without any loss of generality, it may be assumed that $\delta\mathbf{M}$ and $\delta\mathbf{K}$ are zero-mean random matrices. We further assume that the random parts of the system matrices are small and that they also preserve the symmetry, and positive definiteness of the mass matrix, of the perturbed random system. Note that no assumptions on the type of randomness (for example, Gaussian) is made at this stage.

The central aim of studying random eigenvalue problems is to obtain the joint probability density function of the eigenvalues and the eigenvectors. The current literature on random eigenvalue problems in engineering systems is dominated by the mean-centered perturbation methods [20–29]. These methods work well when the uncertainties are small and the parameter distribution is Gaussian. Some researchers have proposed methods that are not based on mean-centered perturbation method. Grigoriu [30] examined the roots of characteristic polynomials of real symmetric random matrices. Recall that eigenvalues are the roots of the characteristic polynomial. Lee and Singh [31] proposed a direct matrix product (Kronecker product) method to obtain the first two moments of the eigenvalues of discrete linear systems. Nair and Keane [32] proposed a stochastic reduced-basis approximation that can be applied to discrete or discretized continuous dynamic systems.

Hála [33] and Mehlhose et al. [34] used a Ritz method to obtain closed-form expressions for moments and probability density functions of the eigenvalues (in terms of Chebyshev–Hermite polynomials). Szekely and Schuëller [35], Pradlwarter et al. [36], and Du et al. [37] considered simulation-based methods to obtain eigensolution statistics of large systems. Ghosh et al. [38] used a polynomial chaos expansion for random eigenvalue problems. Adhikari [39] considered complex random eigenvalue problems associated with nonproportionally damped systems. Verhoosel et al. [40] proposed an iterative method that can be applied to nonsymmetric random matrices also. Rahman [41] developed a dimensional decomposition method for real and complex eigenvalue problems that does not require the calculation of eigensolution derivatives. Recently, Adhikari [42,43] and Adhikari and Friswell [44] have proposed an asymptotic approach to obtain joint and higher-order statistics of the eigenvalues of randomly parametered dynamical systems.

Under special circumstances when the matrix $\mathbf{H} = \mathbf{M}^{-1/2}\mathbf{K}\mathbf{M}^{-1/2} \in \mathbb{R}^{N\times N}$ is Gaussian unitary ensemble or Gaussian orthogonal ensemble, an exact closed-form expression can be obtained for the joint probability density function (pdf) of the eigenvalues using random matrix theory. See Mehta [45] and references therein for discussions on random matrix theory. Random matrix theory has been extended to other type of random matrices. If $\mathbf{H}$ has Wishart distribution then the exact joint pdf of the eigenvalues can be obtained from Muirhead [46] (Theorem 3.2.18). Edelman [47] obtained the pdf of the minimum eigenvalue (first natural frequency squared) of a Wishart matrix. A more general case when the matrix $\mathbf{H}$ has β-distribution has been obtained by Muirhead [46] (Theorem 3.3.4) and, more recently, by Dumitriu and Edelman [48]. Unfortunately the system matrices of real structures may not always follow such distributions and consequently some kind of approximate analysis is required.

In this paper, two experiments are used to study the random eigenvalue analysis methods available in literature. Uncertainties introduced in these experiments are not suitable for applying the stochastic finite element method [2] and related analytical formulations. This is because the stochastic finite element method requires distributed and continuous uncertain parameters (such as the density or Young's modulus of a material). In the experiments proposed here, uncertainties introduced are discrete in nature. As a result, we have used Monte Carlo simulation approach to generate the ensembles of $\delta\mathbf{M}$ and $\delta\mathbf{K}$ and consequently the eigenvalues.

III. Random Eigenvalues of a Fixed–Fixed Beam

A. System Model and Experimental Setup

A steel beam with uniform rectangular cross section is used for the experiment. The details of this experiment have been described by Adhikari et al. [49]. Here, we give a very brief overview. The physical and geometrical properties of the steel beam are: length $L = 1200$ mm, width $b = 40.06$ mm, thickness $t_h = 2.05$ mm, mass density $\rho = 7800\ \mathrm{kg/m^3}$, and Young's modulus $E = 2.0 \times 10^5$ MPa. A steel ruler of length 1.5 m is used for the ease of placing masses at predetermined locations. These locations were generated by a random number generator. The ruler is clamped between 0.05 and 1.25 m so that the effective length of the vibrating beam is 1.2 m. The overall experimental setup is shown in Fig. 1. The end clamps are screwed into two heavy steel blocks, which in turn are fixed to a table with bolts. Twelve equal attachable magnetic masses are used to simulate a randomly varying mass distribution. The magnets are cylindrical in shape and 12.0 mm in length and 6.0 mm in diameter. Some of the attached masses for a sample realization are

[‡]Data available online at http://engweb.swan.ac.uk/~adhikaris/uq/ [retrieved 30 March 2010].

Fig. 1 Test rig for the fixed–fixed beam.

shown in Fig. 2. Each of them weighs 2 g so that the total amount of variable mass is 2.0% of the mass of the beam. The location of the 12 masses are confined to be between 0.2 and 1.0 m of the beam. Hence, a uniform distribution with 100 samples is used to generate the mass locations.

A 32-channel LMS™ system is used to conduct the experiment. In this experiment we used a shaker to act as an impulse hammer. The problem with using the usual manual hammer is that it is in general difficult to hit the beam exactly at the same point with the same amount of force for every sample run. The shaker generates impulses at a pulse rate of 20 s and a pulse width of 0.01 s. Using the shaker in this way we have tried to eliminate any uncertainties arising from the input forces. This innovative experimental technique is designed to ensure that the resulting uncertainty in the response arises purely due to the random locations of the attached masses. We have used a small circular brass plate weighing 2 g to take the impact from the shaker. This was done to hold the accelerometer in the opposite end of the beam via screwing it to the brass plate. This enables us to obtain the driving-point frequency response function. In this experiment three accelerometers are used as the response sensors. The location of the sensors are 23 cm (point 1), 50 cm (point 2, also the actuation point) and 102 cm (point 3) from the left end of the beam. These locations are selected such that two of them are near the two ends of the beam and one is near the middle of the beam. The exact locations are calculated such that the nodal lines of the first few bending modes can be avoided. The steel tip used in the experiment gives clean data up to approximately 4500 Hz. Here, we consider modes up to 1 kHz only. Figure 3 shows the amplitude of the frequency response function (FRF) at points 2 and 3 of the beam without any masses (the baseline model). In the same figure, 100 samples of the amplitude of the FRF are shown together with the ensemble mean, 5, and 95% probability lines. The ensemble mean follows the result of the baseline system closely only in the low-frequency range. The relative variance of the amplitude of the FRF remains more or less constant.

For the random system, an in-house finite element code was developed to implement the discretized version of the equation of motion. Euler–Bernoulli beam element was found to be adequate (the beam is very thin) so that the element stiffness and mass matrices are given by

$$\mathbf{K}_e = \frac{EI}{l^3}\begin{bmatrix} 12 & 6l & -12 & 6l \\ 6l & 4l^2 & -6l & 2l^2 \\ -12 & -6l & 12 & -6l \\ 6l & 2l^2 & -6l & 4l^2 \end{bmatrix} \quad \text{and}$$
$$\mathbf{M}_e = \frac{\rho b t_h l}{420}\begin{bmatrix} 156 & 22l & 54 & -13l \\ 22l & 4l^2 & 13l & -3l^2 \\ 54 & 13l & 156 & -22l \\ -13l & -3l^2 & -22l & 4l^2 \end{bmatrix} \tag{3}$$

where l is the length of an element and $I = bt_h^3/12$ is the moment of inertia of the cross section of the beam. For the numerical calculations 240 elements were used. In the numerical simulation we have included the mass of three accelerometers (6 g each) and the mass of the circular brass plate (2 g). The locations of the randomly attached masses were generated such that they always fall in the nodes of the FE model. This made the calculation of the mass matrix easier in the numerical simulation.

B. Modal Parameter Extraction

There are numerous techniques available for extracting modal parameters from the measured FRF data [19]. In general, these methods may be classified as single-degree-of-freedom methods or multiple-degree-of-freedom (MDOF) methods, depending upon whether one chooses to fit a curve to a single mode or to multiple modes. Because of the large number of modes observed in the frequency range of interest, selection of an MDOF technique is preferred. In the present work, the RFP method and an NLS technique are used in this paper.

The RFP method is based on writing the FRF as a ratio of two polynomials $N(\omega)$ and $D(\omega)$, i.e., $H(\omega) = N(\omega)/D(\omega)$. The zeros of the denominator $D(\omega)$ give the natural frequencies and damping factors. The value of the numerator polynomial ($N(\omega)$) at the natural frequency gives the residue for that mode. The mode shapes are

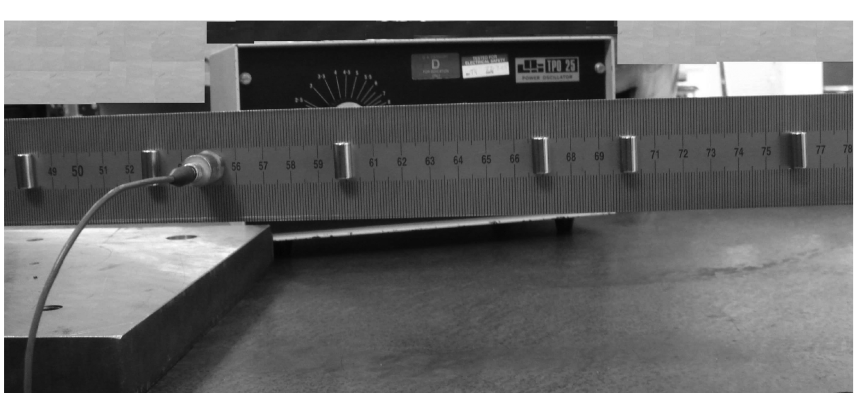

Fig. 2 Attached masses (magnets) at random locations. In total, 12 masses, each weighing 2 g, are used.

obtained from the fitted residues. A detailed description of this method can be found in [19,50,51]. In this paper, the MATLAB™ function invfreqs is used to fit a rational fraction polynomial to the FRF data. The rational fraction polynomial method implemented here can identify more than one mode from a single FRF measurement. However, this method identifies spurious peaks or computational modes that do not physically correspond to any resonant mode. To avoid this, the RFP method was used to fit a portion of measured FRF data around a single mode. By doing so, one can ensure that a single, physically meaningful, resonant peak is fitted. The nonlinear least-squares method is more advantageous from this perspective.

The problem of estimating complex poles and residues from FRFs is nonlinear in general [52–54]. However, if the poles are known, estimating residues can be simplified to a linear least-squares problem. Based on a Levenberg–Marquardt algorithm described in [55], the nonlinear least-squares method used here was developed by Duffour [56]. The full nonlinear least-squares problem of fitting the modal parameters to the FRF data is solved based on a set of initial guesses for natural frequencies and damping factors provided by the RFP method. The principal advantage of the nonlinear least-squares method is that several FRFs corresponding to different excitation/measurement locations on the test structure can be fitted in one stage, instead of fitting each FRF separately. Thus, the best global estimates

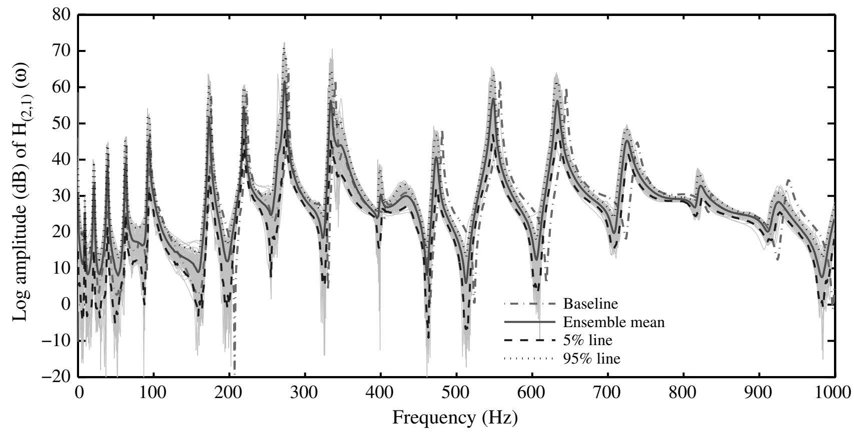

a) Point 1 (23 cm from the left end)

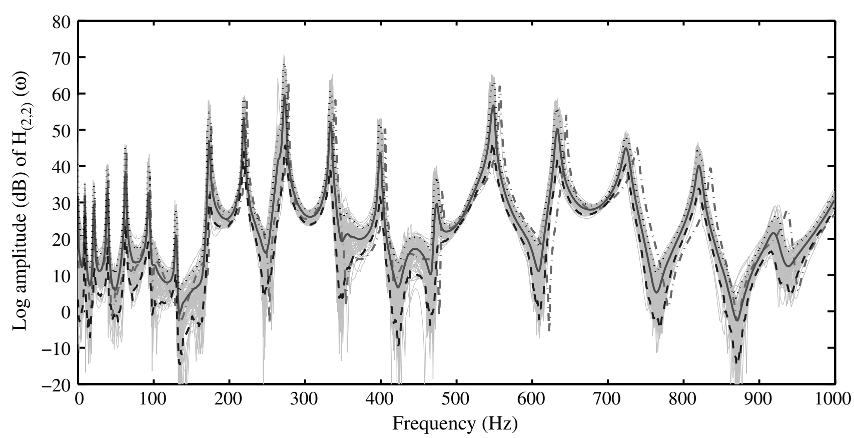

b) Point 2 (the driving point FRF, 50 cm from the left end)

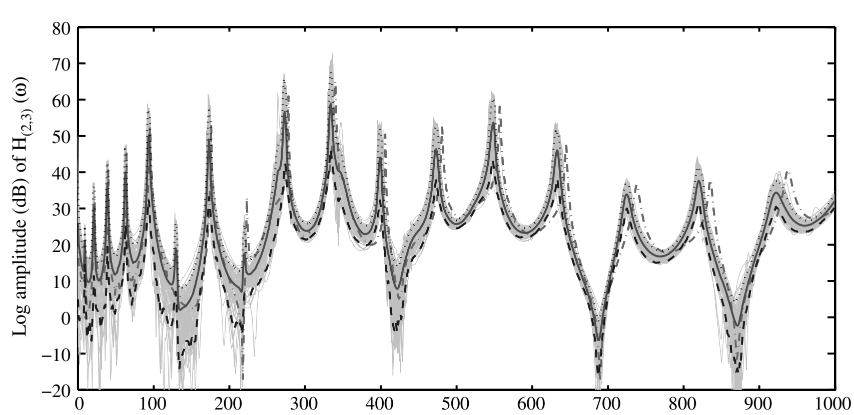

c) Point 3 (102 cm from the left end)

Fig. 3 Measured amplitudes of the driving-point FRF and a cross FRF of the beam with 12 randomly placed masses: 100 FRFs, together with the ensemble mean, 5, and 95% probability points.

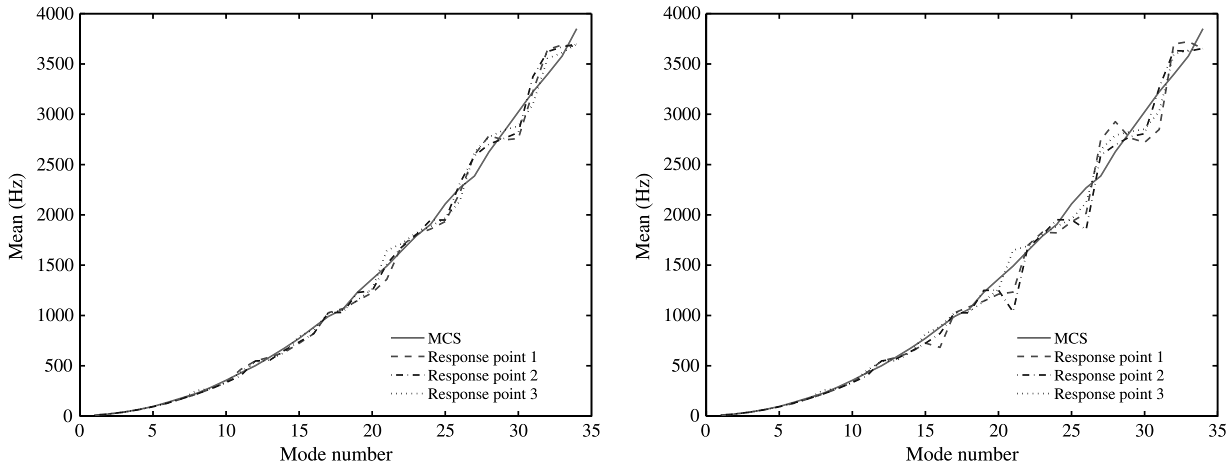

a) Rational fraction polynomial method **b)Nonlinear least-squares method**

Fig. 4 Comparison of the mean of the natural frequencies of the fixed–fixed beam obtained using the direct Monte Carlo simulation (MCS) and experimental results extracted using two different methods.

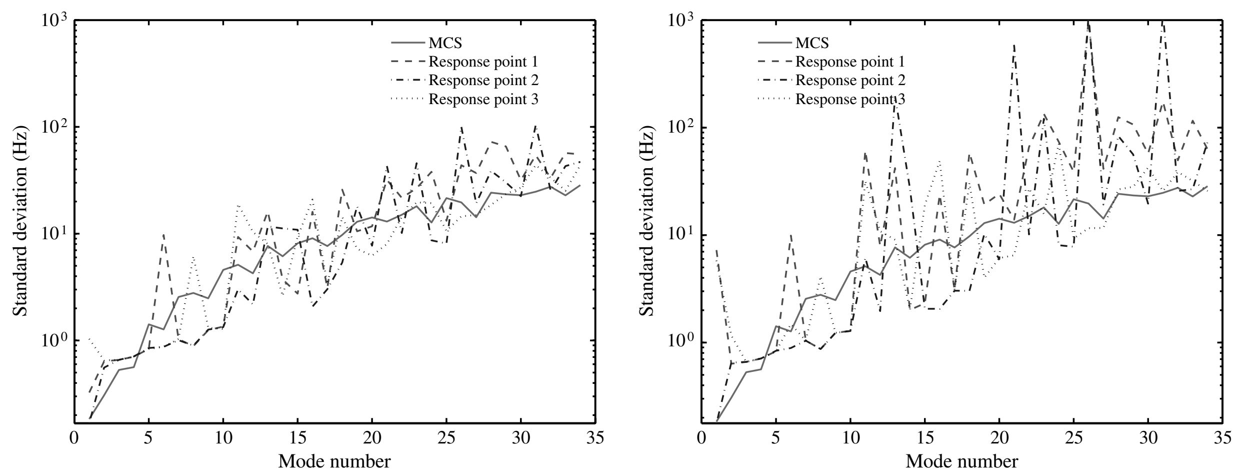

a) Rational fraction polynomial method **b) Nonlinear least-squares method**

Fig. 5 Comparison of the standard deviation of the natural frequencies of the fixed–fixed beam obtained using the direct Monte Carlo simulation and experimental results extracted using two different methods.

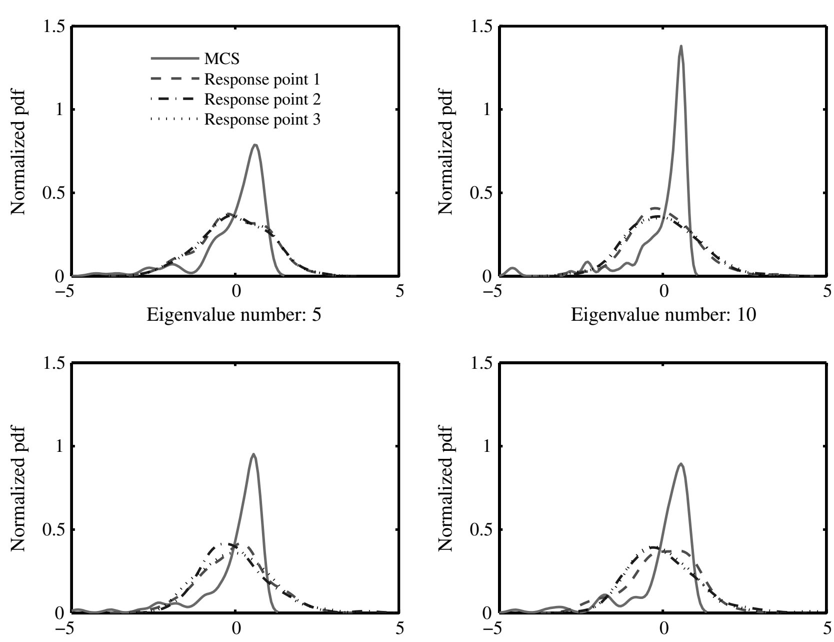

Fig. 6 Comparison of the probability density functions of four selected natural frequencies of the fixed–fixed beam obtained using the direct Monte Carlo simulation and experimental results extracted using the rational fraction polynomial method.

of the natural frequencies and damping factors can be obtained by using this method. The above two methods of modal parameter extraction were used in estimating the natural frequencies and damping factors from the measured FRF data.

C. Eigenvalue Statistics

The detailed statistical analysis of the natural frequencies and comparison with analytical method is shown in Figs. 4–7. The baseline model of the beam does not have any attached masses. As a result, the natural frequencies of the random systems consisting of 12 masses have lower frequencies compared with the baseline model. This can be clearly seen in the left shift of the resonance peaks of the ensemble mean corresponding to the random systems with respect to the baseline system in Fig. 3. The numerical values behind these plots are given in Table 1 for the purpose of possible comparisons using other analytical methods not considered in our paper. In these figures, the indicated system identification method was used to extract the natural frequencies within 2 kHz from the frequency responses measured at three different spatial points on the beam. The ensemble statistics for each spatial location and for each identification method can be compared via Figs. 4 and 5. In Fig. 4 the ensemble mean calculated from the *identified* natural frequencies from *measured* frequency response functions, are compared with the Monte Carlo simulations. It is instructive to compare the degree of agreement obtained by the two methods and the variation in mean with spatial location of the sensor or response measurement point. Significant differences in the mean for the three response points can be observed in the high-frequency regime. It can also be seen that the *global* nonlinear least-squares method exhibits significant variability. This is also reflected in Fig. 5.

The normalized probability density function (pdf) plots shown in Figs. 6 and 7 compare the Monte Carlo simulation results with experimental data. Suppose ω_j is the random variable describing the jth natural frequency with mean $\bar{\omega}_j$ and standard deviation σ_{ω_j}. In these plots, we have normalized the natural frequencies as

$$\tilde{\omega}_j = \frac{\omega_j - \bar{\omega}_j}{\sigma_{\omega_j}} \tag{4}$$

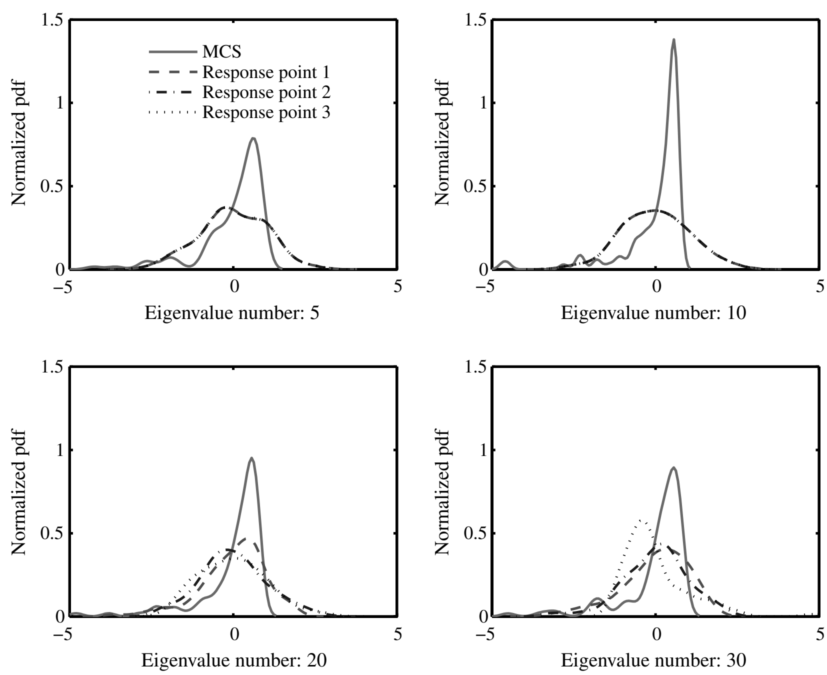

Fig. 7 Comparison of the probability density functions of four selected natural frequencies of the fixed–fixed beam obtained using the direct Monte Carlo simulation and experimental results extracted using the nonlinear least-squares method.

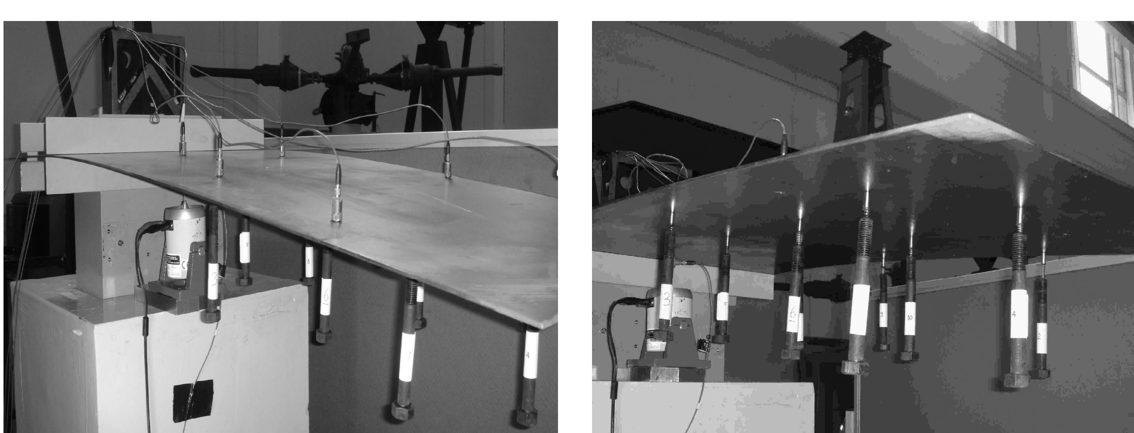

a) Experimental setup showing the accelerometer locations

b) Experimental setup showing a realization of the attached oscillators

Fig. 8 Test rig for the cantilever plate: position of the shaker (used as a impact hammer), a sample of the attached oscillators, and the accelerometers.

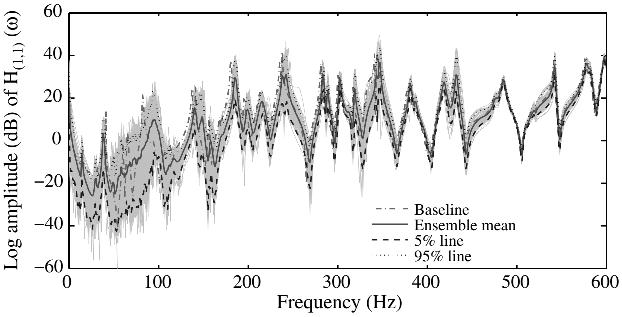

a) Point 1 (nodal coordinate: (4,6), driving point FRF)

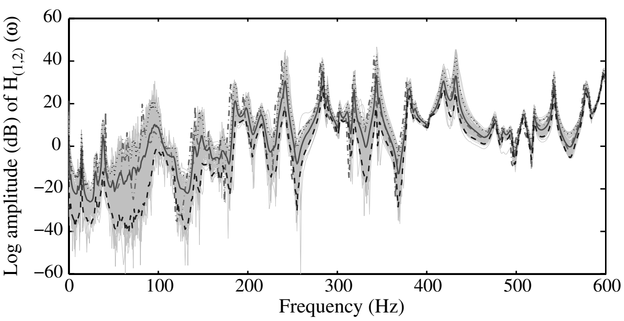

b) Point 2 (nodal coordinate: (6,11)

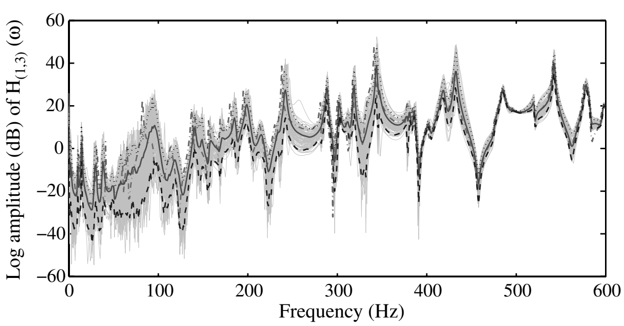

c) Point 3 (nodal coordinate: (11,3))

Fig. 9 Measured amplitudes of the FRF of the plate with 10 randomly placed oscillators: 100 FRFs, together with the ensemble mean, 5, and 95% probability points.

The main reason behind considering the normalized pdf plots is to qualitatively understand whether the experimental pdfs are close to the Gaussian pdf, an assumption often made in many analytical approaches. This can be best achieved across different frequencies when the data is normalized. Such normalization can qualitatively confirm whether the Gaussian assumption is justified. Recently, Goyal and Kapania [57] have used a similar nondimensional approach for stochastic stability analysis of composite beams. The quantitative values of the means and standard deviations corresponding to the found natural frequencies selected here can be seen in Figs. 4 and 5.

The increasing variability is obvious as one proceeds higher in the mode sequence. The agreement at the level of pdfs is far from satisfactory. This suggests that even though the first two moments can be predicted with reasonable accuracy using Monte Carlo simulations the higher moments may not agree. Although experimentally measured normalized pdfs are closer to Gaussian ensemble, albeit with nonzero mean, the Monte Carlo simulations are not.

IV. Random Eigenvalues of a Cantilever Plate

A. System Model and Experimental Setup

We consider the dynamics of a steel cantilever plate with homogeneous geometric (i.e., uniform thickness) and constitutive properties (i.e., uniform Young's modulus and Poisson's ratio). The baseline model is perturbed by a set of spring-mass oscillators of different natural frequencies attached randomly along the plate. The aim of this experiment is to simulate uncertain unmodeled dynamics. The details of this experiment has been described by Adhikari et al. [49,58]. Here, we give a very brief overview. The test rig has been designed for simplicity and ease of replication and modeling. The overall arrangement of the test rig is shown in Fig. 8. A rectangular steel plate with uniform thickness is used for the experiment. The physical and geometrical properties of the steel plate are assumed to be $E = 200 \times 10^9\ \mathrm{N/m^2}$, $\mu = 0.3$, $\rho = 7860\ \mathrm{kg/m^3}$, $t_h = 3.0$ mm, $L_x = 0.998$ m, and $L_y = 0.59$ m. The plate is clamped along one edge using a clamping device. The clamping device is attached on the top of a heavy concrete block and the whole assembly is placed on a steel table. The plate weighs about 12.28 kg and special care has been taken to ensure its stability and minimizing the vibration transmission. The plate is divided into 375 elements (25 along the length and 15 along the width). Assuming one corner on the cantilevered edge as the origin, we have assigned coordinates to all the nodes. Oscillators and accelerometers are attached on these nodes. This has been done to ease finite element modeling. The bottom surface of the plate is marked with node numbers so that the oscillators can be hung at the nodal locations. This scheme is aimed at reducing uncertainly arising from the measurement of the locations of the oscillators. A discrete random number generator is used to generate the X and Y coordinates of the oscillators. In total, 10 oscillators are used to simulate random unmodeled dynamics. The spring is glue-welded with a magnet at the top and a mass at the bottom. The magnet at the top of the assembly helps to attach the

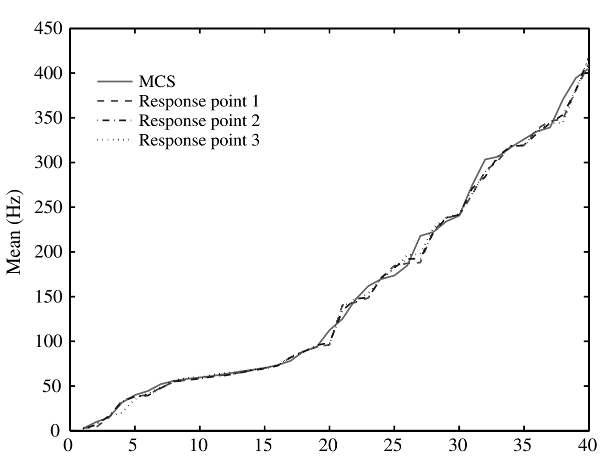

a) Rational fraction polynomial method

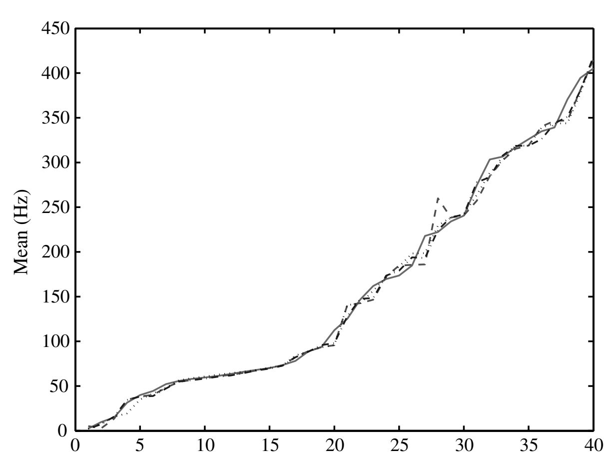

b) Nonlinear least-squares method

Fig. 10 Comparison of the mean of the natural frequencies of the fixed–fixed plate obtained using the direct Monte Carlo simulation and experimental results extracted using two different methods.

oscillators at the bottom of the plate repeatedly without much difficulty. The stiffness of the 10 springs used in the experiment are 16.800, 09.100, 17.030, 24.000, 15.670, 22.880, 17.030, 22.880, 21.360, and 19.800 kN/m. The oscillating mass of each of the 10 oscillators is 121.4 g. Therefore, the total oscillating mass is 1.214 kg, which is 9.8% of the mass of the plate. The natural frequencies of the 10 oscillators are obtained as 59.2060 43.5744, 59.6099, 70.7647, 57.1801, 69.0938, 59.6099, 69.0938, 66.7592, and 64.2752 Hz. The springs are attached to the plate at the pregenerated nodal locations using the small magnets located at the top the assembly. The small magnets (weighing 2 g) are found to be strong enough to hold the 121.4 g mass attached to the spring below over the frequency range considered. One hundred realizations of attached oscillators are created (by hanging the oscillators at random locations) and tested individually in this experiment.

The 32-channel LMS™ system used in the beam experiment is again employed for this experiment. The shaker is placed so that it impacts at the (4,6) node of the plate. In this experiment six accelerometers are used as the response sensors. The locations of the six sensors are selected such that they cover a broad area of the plate. The locations of the accelerometers can be seen in Fig. 8. The nodal locations of the accelerometers are as follows: point 1 is (4,6), point 2 is (6,11), point 3 is (11,3), point 4 is (14,14), point 5 is (18,2), and point 6 is (21,10). Small holes are drilled into the plate and all of the six accelerometers are attached by screwing through the holes. We consider modes up to 600 Hz. Figure 9 shows the amplitude of the frequency response function (FRF) at points 1, 2, and 3 of the plate without any masses (the baseline model). The measured FRFs have frequency resolution of 1 Hz. In the same figure, 100 samples of the amplitude of the FRF are shown together with the ensemble mean, 5, and 95% probability lines. The ensemble mean follows the result of the baseline system closely only in the low-frequency range. The relative variance of the amplitude of the FRF remains more or less constant.

For this random system, an in-house finite element code was developed. We considered a rectangular thin plate element with 3 degrees of freedom per node (rotations in x, y and deflection in z direction). The 12×12 element stiffness and mass matrices were obtained following the standard finite element method [59]. This simple model neglects the shear deformation and therefore

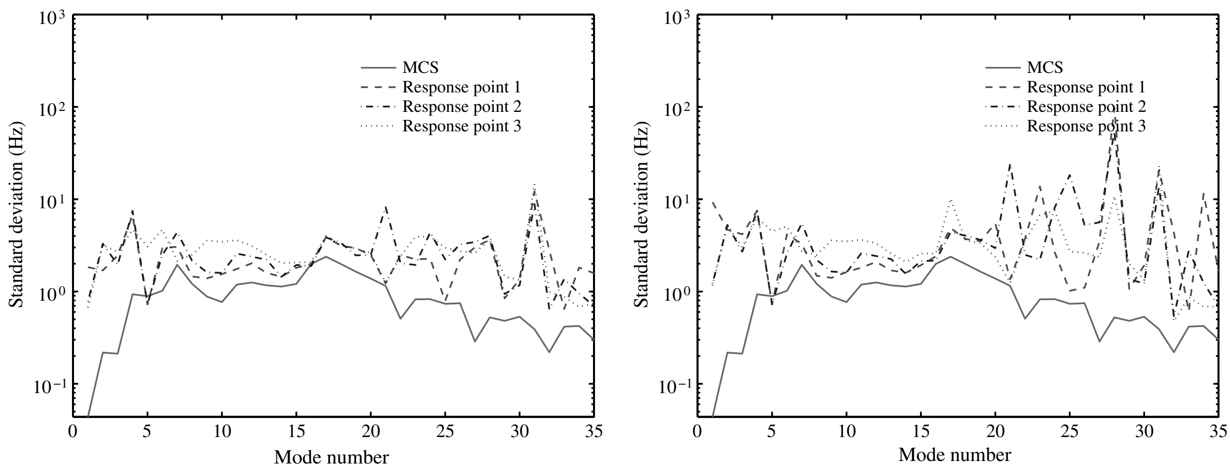

a) Rational fraction polynomial method   b) Nonlinear least-squares method

Fig. 11 Comparison of the standard deviation of the natural frequencies of the fixed–fixed plate obtained using the direct Monte Carlo simulation and experimental results extracted using two different methods.

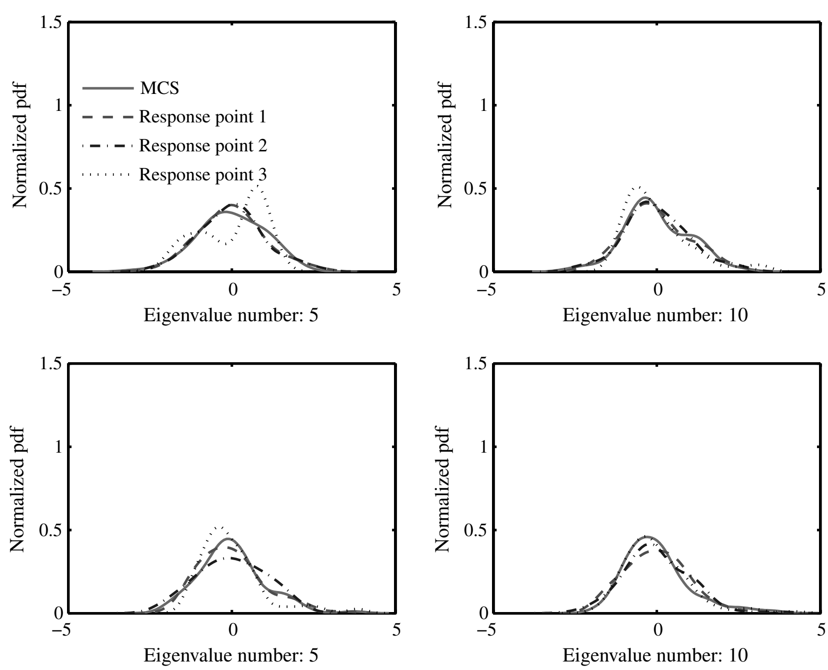

Fig. 12 Comparison of the probability density functions of four selected natural frequencies of the fixed–fixed plate obtained using the direct Monte Carlo simulation and experimental results extracted using the rational fraction polynomial method.

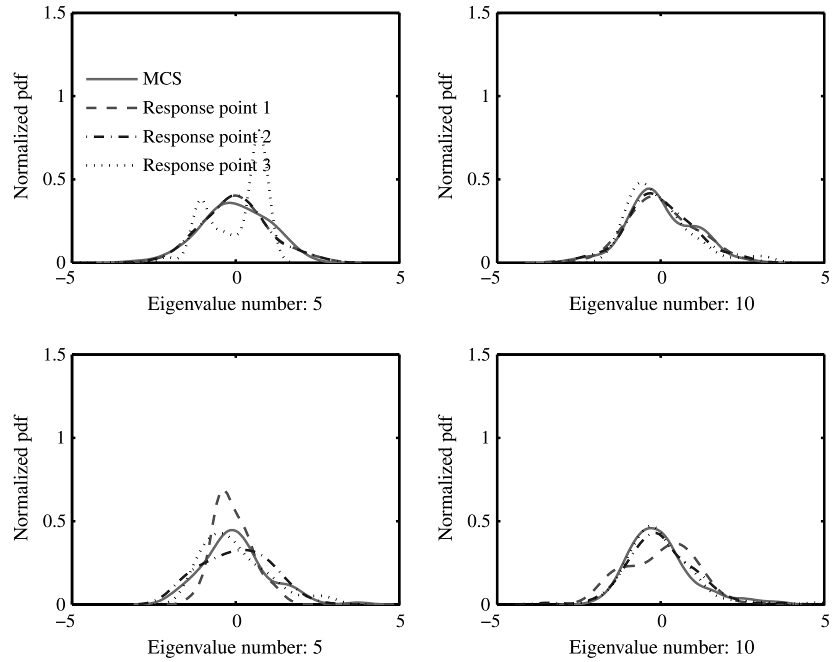

Fig. 13 Comparison of the probability density functions of four selected natural frequencies of the fixed–fixed plate obtained using the direct Monte Carlo simulation and experimental results extracted using the nonlinear least-squares method.

may not be suitable for very-high-frequency regime. Mass of the accelerometers are used in the model. The meshing was done in such a away (in the multiple of a 25 × 15 grid) that the attached oscillators always fall in the nodes. This makes the assembly of the global matrices simpler in the in-house code.

B. Eigenvalue Statistics

We used the same modal parameter estimation techniques as in the case of the beam: namely, RFP method and nonlinear least-squares method. The high modal density, or closely spaced modes, is a particular feature associated with plate experimental data. The

Table 1 Mean and standard deviation of identified natural frequencies of the fixed–fixed beam (in hertz) from the measured FRFs at three spatial locations using two identification methods

	Rational fraction polynomial			Nonlinear least-squares		
Mode	FRF 1	FRF 2	FRF 3	FRF 1	FRF 2	FRF 3
1	9.08 ± 0.33	9.24 ± 0.17	8.39 ± 1.03	10.07 ± 7.25	9.26 ± 0.18	6.73 ± 5.79
2	21.03 ± 0.64	20.89 ± 0.56	21.01 ± 0.65	21.04 ± 0.63	20.92 ± 0.65	21.08 ± 1.16
3	38.94 ± 0.66	38.92 ± 0.66	38.93 ± 0.66	38.94 ± 0.66	38.92 ± 0.66	38.93 ± 0.66
4	62.83 ± 0.70	62.81 ± 0.71	62.80 ± 0.71	62.80 ± 0.71	62.79 ± 0.71	62.79 ± 0.71
5	93.79 ± 0.84	93.47 ± 0.85	93.65 ± 0.83	93.68 ± 0.83	93.58 ± 0.84	93.64 ± 0.83
6	128.37 ± 9.71	129.56 ± 0.87	129.50 ± 0.87	125.96 ± 9.89	129.80 ± 0.89	129.65 ± 1.49
7	173.12 ± 1.03	173.50 ± 1.01	173.09 ± 1.03	173.07 ± 1.04	173.10 ± 1.04	173.06 ± 1.04
8	219.27 ± 0.89	219.08 ± 0.90	254.58 ± 6.15	219.15 ± 0.87	219.13 ± 0.87	258.00 ± 4.14
9	273.25 ± 1.25	273.27 ± 1.26	273.34 ± 1.32	273.21 ± 1.23	273.21 ± 1.23	273.20 ± 1.23
10	333.73 ± 1.35	333.93 ± 1.33	333.59 ± 1.28	333.70 ± 1.28	333.66 ± 1.28	333.68 ± 1.28
11	463.00 ± 9.33	400.79 ± 3.01	437.50 ± 19.02	433.38 ± 61.23	399.88 ± 6.15	453.62 ± 31.80
12	547.08 ± 6.82	547.82 ± 2.17	536.75 ± 10.36	547.19 ± 7.91	548.06 ± 1.96	546.44 ± 10.87
13	586.51 ± 16.17	556.38 ± 11.69	558.63 ± 7.99	582.26 ± 42.03	568.49 ± 197.38	549.63 ± 9.04
14	633.64 ± 3.73	653.19 ± 11.19	632.86 ± 2.61	633.24 ± 2.01	642.32 ± 27.31	633.09 ± 2.02
15	723.71 ± 2.75	736.54 ± 10.88	793.22 ± 9.38	725.60 ± 2.32	723.90 ± 2.06	816.57 ± 19.01
16	818.82 ± 16.02	819.59 ± 2.08	858.80 ± 20.83	683.02 ± 23.78	820.44 ± 2.06	890.44 ± 49.07
17	1027.30 ± 3.11	1026.88 ± 3.02	1024.12 ± 3.38	1026.92 ± 3.09	1026.66 ± 3.04	1026.59 ± 3.05
18	1067.56 ± 25.85	1030.01 ± 5.37	1053.84 ± 14.38	1086.05 ± 58.56	1026.59 ± 3.02	1037.18 ± 30.62
19	1147.37 ± 10.53	1227.66 ± 18.04	1153.54 ± 7.22	1142.98 ± 19.27	1249.20 ± 10.22	1140.21 ± 4.01
20	1226.03 ± 11.72	1247.07 ± 7.73	1262.04 ± 6.23	1211.84 ± 24.22	1251.38 ± 5.97	1259.83 ± 6.10
21	1359.68 ± 31.90	1511.76 ± 43.04	1645.14 ± 8.01	1232.35 ± 13.91	1036.05 ± 579.58	1648.12 ± 6.48
22	1688.71 ± 21.69	1676.45 ± 10.16	1713.01 ± 14.35	1695.06 ± 65.95	1673.54 ± 10.14	1689.50 ± 27.14
23	1805.43 ± 26.70	1799.71 ± 45.71	1818.78 ± 19.62	1826.81 ± 134.14	1800.18 ± 120.84	1807.81 ± 15.71
24	1858.83 ± 38.02	1948.64 ± 8.67	1884.30 ± 19.30	1820.68 ± 73.88	1952.01 ± 8.05	1886.24 ± 70.76
25	1933.49 ± 13.20	1949.28 ± 8.10	1967.87 ± 10.65	1932.16 ± 38.74	1951.21 ± 7.78	1957.80 ± 9.30
26	2220.78 ± 43.82	2315.33 ± 100.49	2136.00 ± 14.54	2015.97 ± 998.14	1854.72 ± 1114.61	2122.31 ± 11.61
27	2597.18 ± 37.01	2585.93 ± 19.24	2623.51 ± 14.99	2745.13 ± 41.36	2592.98 ± 19.24	2647.11 ± 11.64
28	2787.48 ± 72.53	2703.42 ± 38.82	2774.62 ± 18.57	2926.50 ± 125.09	2695.32 ± 83.54	2790.94 ± 26.63
29	2744.54 ± 65.69	2758.39 ± 30.22	2841.25 ± 23.53	2765.70 ± 106.87	2776.99 ± 56.24	2828.18 ± 28.11
30	2759.01 ± 31.72	2819.70 ± 22.43	2883.49 ± 27.00	2719.83 ± 57.31	2806.86 ± 19.61	2852.38 ± 42.42
31	3227.53 ± 54.19	3373.65 ± 104.31	3099.94 ± 43.95	2849.03 ± 175.06	3263.22 ± 1163.50	3028.99 ± 25.66
32	3643.10 ± 33.30	3623.34 ± 25.36	3554.33 ± 33.42	3697.44 ± 49.57	3633.21 ± 25.76	3598.47 ± 38.64
33	3689.33 ± 56.99	3669.52 ± 43.03	3611.74 ± 25.31	3722.14 ± 116.06	3626.82 ± 26.75	3634.27 ± 31.89
34	3672.02 ± 55.41	3698.77 ± 47.02	3698.47 ± 43.93	3651.91 ± 62.85	3655.25 ± 73.61	3652.49 ± 25.76

Table 2 Mean and standard deviation of identified natural frequencies of the cantilevered plate (in hertz) from the measured FRFs at six spatial locations using two identification methods

	Rational fraction polynomial						Nonlinear least-squares					
Mode	FRF 1	FRF 2	FRF 3	FRF 4	FRF 5	FRF 6	FRF 1	FRF 2	FRF 3	FRF 4	FRF 5	FRF 6
1	3.19 ± 1.84	2.00 ± 0.78	2.10 ± 0.67	2.15 ± 0.40	2.14 ± 0.46	2.19 ± 0.23	5.20 ± 9.29	2.06 ± 1.22	2.17 ± 1.16	2.21 ± 0.58	2.12 ± 0.57	2.21 ± 0.22
2	3.75 ± 1.69	6.55 ± 3.30	7.17 ± 3.19	7.19 ± 3.15	5.89 ± 2.86	4.32 ± 2.50	2.70 ± 4.67	7.33 ± 5.24	8.06 ± 5.25	7.85 ± 4.88	5.84 ± 3.39	4.15 ± 2.96
3	14.83 ± 2.45	16.39 ± 1.94	16.43 ± 2.68	17.05 ± 2.62	12.78 ± 2.51	16.25 ± 2.49	13.47 ± 4.16	15.85 ± 2.70	15.48 ± 3.01	16.68 ± 4.54	12.74 ± 3.88	15.62 ± 2.71
4	33.64 ± 6.71	32.52 ± 7.46	20.29 ± 4.67	24.02 ± 5.42	36.01 ± 4.63	22.35 ± 6.94	34.63 ± 7.50	34.47 ± 7.48	19.59 ± 6.33	24.21 ± 8.07	37.03 ± 4.70	22.29 ± 7.70
5	38.30 ± 0.72	38.26 ± 0.73	35.43 ± 3.08	36.83 ± 2.41	38.31 ± 0.73	35.73 ± 2.91	38.30 ± 0.72	38.30 ± 0.73	34.85 ± 4.50	36.90 ± 2.97	38.31 ± 0.73	35.78 ± 3.12
6	40.23 ± 2.95	39.33 ± 2.50	41.97 ± 4.68	41.85 ± 4.20	39.91 ± 3.06	42.77 ± 4.41	40.20 ± 4.16	38.86 ± 2.58	41.53 ± 5.08	41.31 ± 5.66	39.29 ± 3.09	42.74 ± 4.47
7	48.08 ± 3.05	47.67 ± 4.38	48.45 ± 2.15	50.04 ± 3.52	48.65 ± 3.06	50.07 ± 2.49	48.02 ± 3.28	47.23 ± 5.48	48.20 ± 2.72	50.25 ± 3.84	47.75 ± 4.39	50.12 ± 2.69
8	54.67 ± 1.45	54.94 ± 2.15	56.29 ± 2.49	55.07 ± 1.68	54.40 ± 1.59	54.38 ± 2.33	54.70 ± 1.48	54.96 ± 2.19	56.32 ± 2.50	55.13 ± 1.67	54.44 ± 1.67	54.38 ± 2.35
9	56.82 ± 1.39	56.53 ± 1.61	58.80 ± 3.55	56.37 ± 1.62	56.87 ± 3.03	56.98 ± 1.80	56.82 ± 1.41	56.57 ± 1.65	58.78 ± 3.57	56.31 ± 1.72	56.91 ± 3.08	56.96 ± 1.85
10	58.64 ± 1.54	58.29 ± 1.59	60.59 ± 3.46	57.76 ± 1.73	58.86 ± 2.73	58.70 ± 2.76	58.61 ± 1.62	58.26 ± 1.61	60.61 ± 3.49	57.74 ± 1.76	58.82 ± 2.76	58.70 ± 2.77
11	60.85 ± 1.75	60.45 ± 2.58	62.77 ± 3.60	59.86 ± 3.22	60.75 ± 3.26	60.22 ± 3.49	60.87 ± 1.82	60.42 ± 2.59	62.76 ± 3.63	59.87 ± 3.24	60.76 ± 3.28	60.22 ± 3.49
12	62.51 ± 2.02	61.87 ± 2.39	64.39 ± 3.13	62.28 ± 3.06	62.78 ± 3.56	62.05 ± 3.99	62.54 ± 2.09	61.84 ± 2.42	64.39 ± 3.32	62.29 ± 3.08	62.75 ± 3.57	62.03 ± 4.00
13	64.81 ± 1.59	64.42 ± 2.21	66.21 ± 2.49	64.62 ± 2.83	65.58 ± 3.01	64.96 ± 5.04	64.83 ± 1.69	64.46 ± 2.25	66.20 ± 2.58	64.68 ± 2.94	65.57 ± 3.05	64.94 ± 5.05
14	67.42 ± 1.44	67.36 ± 1.44	67.84 ± 2.03	67.22 ± 3.14	67.84 ± 2.07	67.64 ± 2.01	67.42 ± 1.59	67.41 ± 1.54	67.85 ± 2.09	67.25 ± 3.16	67.90 ± 2.23	67.55 ± 2.17
15	70.06 ± 1.81	69.47 ± 1.94	70.34 ± 2.07	69.84 ± 1.99	70.32 ± 2.06	70.34 ± 1.89	70.08 ± 1.93	69.48 ± 2.13	70.55 ± 2.59	69.85 ± 2.10	70.39 ± 2.17	70.39 ± 2.07
16	72.72 ± 1.99	72.75 ± 1.89	72.84 ± 2.08	72.60 ± 1.69	72.60 ± 1.94	72.70 ± 1.68	72.92 ± 2.40	72.75 ± 2.16	73.01 ± 2.57	72.66 ± 1.99	72.71 ± 2.28	72.69 ± 1.82
17	82.02 ± 3.88	81.77 ± 3.85	82.46 ± 4.05	81.62 ± 3.76	82.72 ± 3.88	82.12 ± 3.69	82.54 ± 4.87	82.17 ± 4.39	84.01 ± 10.13	81.93 ± 6.00	83.16 ± 4.38	82.52 ± 4.10
18	88.69 ± 3.13	88.22 ± 3.36	88.81 ± 3.16	88.38 ± 3.23	88.50 ± 3.19	88.82 ± 2.92	88.98 ± 3.70	88.45 ± 4.02	88.95 ± 3.55	88.85 ± 3.72	88.84 ± 3.59	89.03 ± 3.21
19	93.78 ± 2.95	95.53 ± 2.46	93.77 ± 2.92	97.21 ± 3.53	93.80 ± 2.82	95.42 ± 2.76	93.55 ± 3.51	95.74 ± 3.63	93.31 ± 3.34	97.33 ± 4.06	93.10 ± 3.55	95.06 ± 4.23
20	96.03 ± 2.49	98.41 ± 2.50	96.57 ± 2.62	101.05 ± 4.77	97.96 ± 4.14	98.75 ± 3.15	95.64 ± 5.47	98.02 ± 2.95	95.92 ± 2.37	99.87 ± 5.06	97.27 ± 4.80	98.66 ± 3.49
21	140.54 ± 1.22	134.24 ± 8.22	140.56 ± 1.25	138.27 ± 3.84	134.60 ± 8.14	140.32 ± 0.94	140.44 ± 1.36	128.07 ± 24.26	140.59 ± 1.24	140.22 ± 2.40	133.83 ± 11.95	140.38 ± 1.01
22	143.52 ± 2.48	147.48 ± 2.03	144.30 ± 2.41	144.15 ± 2.12	147.54 ± 1.68	141.92 ± 1.63	142.70 ± 3.74	147.62 ± 2.50	142.18 ± 3.55	142.28 ± 3.36	147.49 ± 1.71	140.70 ± 1.56
23	148.65 ± 2.23	149.13 ± 1.94	153.97 ± 3.90	152.62 ± 3.33	149.38 ± 3.45	156.35 ± 4.96	146.52 ± 13.76	148.34 ± 2.21	156.70 ± 6.68	152.25 ± 4.87	149.06 ± 5.50	161.93 ± 7.64
24	171.01 ± 2.26	171.37 ± 4.38	169.57 ± 3.95	169.61 ± 2.67	170.61 ± 2.07	170.04 ± 1.99	172.61 ± 2.65	173.47 ± 8.18	171.27 ± 7.50	169.56 ± 3.19	170.28 ± 2.39	170.17 ± 2.31
25	184.50 ± 0.79	182.59 ± 2.22	181.63 ± 2.98	181.74 ± 2.65	184.44 ± 1.02	178.17 ± 5.33	184.73 ± 1.02	179.06 ± 18.24	183.58 ± 2.71	184.01 ± 2.09	184.88 ± 1.09	180.94 ± 6.95
26	187.18 ± 2.22	192.04 ± 3.24	196.62 ± 2.73	188.23 ± 2.74	187.69 ± 2.52	195.49 ± 5.30	185.53 ± 1.10	193.95 ± 5.24	198.32 ± 2.62	186.65 ± 4.07	186.07 ± 3.15	197.08 ± 6.25
27	188.03 ± 3.01	192.60 ± 3.44	197.35 ± 2.62	189.16 ± 3.15	188.71 ± 3.15	198.37 ± 5.99	186.04 ± 3.48	193.21 ± 5.62	198.55 ± 2.36	188.21 ± 5.98	187.48 ± 5.44	200.87 ± 8.90
28	223.25 ± 3.66	221.21 ± 4.03	226.86 ± 3.67	233.25 ± 1.83	219.26 ± 3.16	225.52 ± 2.47	259.90 ± 97.52	224.38 ± 54.63	229.32 ± 10.80	234.28 ± 1.90	217.08 ± 2.88	225.54 ± 3.94
29	238.26 ± 0.84	238.17 ± 0.94	238.35 ± 1.45	237.74 ± 1.07	237.64 ± 0.96	236.55 ± 1.62	238.37 ± 1.07	238.62 ± 1.35	238.73 ± 2.00	238.05 ± 1.15	237.95 ± 1.52	237.26 ± 1.94
30	240.77 ± 1.36	241.51 ± 1.17	242.38 ± 1.33	240.54 ± 1.38	239.46 ± 1.47	240.37 ± 1.41	240.82 ± 1.92	241.81 ± 1.22	242.06 ± 1.33	240.62 ± 1.96	238.86 ± 2.61	240.26 ± 2.12
31	264.14 ± 12.14	270.95 ± 8.85	265.03 ± 14.55	266.92 ± 9.79	284.52 ± 3.00	280.42 ± 11.11	257.26 ± 20.54	277.81 ± 13.91	263.77 ± 23.16	261.86 ± 20.79	285.15 ± 2.65	281.45 ± 15.79
32	290.04 ± 2.81	283.84 ± 0.64	289.60 ± 0.99	284.44 ± 0.85	287.13 ± 1.12	292.85 ± 2.31	284.72 ± 4.34	283.59 ± 0.54	288.43 ± 0.48	283.65 ± 0.55	287.68 ± 1.58	292.05 ± 8.07
33	302.40 ± 0.65	307.28 ± 1.36	304.05 ± 0.88	306.73 ± 1.18	304.92 ± 2.44	302.19 ± 0.55	302.35 ± 0.61	307.68 ± 2.77	302.58 ± 0.87	307.33 ± 1.97	305.20 ± 4.84	302.24 ± 0.53
34	318.38 ± 1.82	318.40 ± 0.95	318.69 ± 0.68	313.88 ± 3.36	317.95 ± 0.77	318.09 ± 1.04	315.37 ± 11.48	318.58 ± 1.24	318.74 ± 0.69	309.40 ± 4.91	318.46 ± 1.20	318.36 ± 1.30
35	319.27 ± 1.58	318.86 ± 0.70	318.81 ± 0.74	323.44 ± 4.69	318.68 ± 0.66	322.14 ± 3.70	318.88 ± 1.65	318.77 ± 0.68	318.76 ± 0.68	327.58 ± 13.41	318.70 ± 0.68	324.01 ± 7.08
36	337.59 ± 1.92	332.69 ± 4.19	336.60 ± 2.73	335.05 ± 4.12	330.33 ± 6.25	335.76 ± 3.73	340.21 ± 1.67	326.16 ± 42.05	338.87 ± 3.56	337.21 ± 12.24	327.91 ± 23.58	336.80 ± 16.89
37	346.13 ± 0.60	343.81 ± 0.73	343.84 ± 0.70	345.31 ± 0.82	350.00 ± 4.73	346.32 ± 0.57	346.56 ± 0.53	343.75 ± 0.84	343.74 ± 0.80	345.82 ± 1.43	364.38 ± 10.59	346.58 ± 0.49
38	348.67 ± 3.42	353.39 ± 8.05	344.20 ± 0.82	347.75 ± 3.12	383.36 ± 1.55	346.57 ± 0.56	346.91 ± 3.46	351.19 ± 15.25	343.78 ± 0.84	346.24 ± 1.49	384.73 ± 2.50	346.59 ± 0.49
39	381.39 ± 0.57	380.99 ± 0.62	381.74 ± 1.50	384.79 ± 0.33	384.62 ± 0.93	384.97 ± 2.36	381.10 ± 0.52	380.56 ± 0.69	377.15 ± 2.70	385.70 ± 0.40	385.57 ± 1.72	390.21 ± 13.08
40	410.08 ± 1.29	418.03 ± 1.44	416.60 ± 0.88	412.82 ± 3.87	416.36 ± 8.09	416.76 ± 0.67	415.09 ± 0.34	418.46 ± 1.24	418.04 ± 0.88	415.72 ± 10.88	427.26 ± 12.84	417.17 ± 0.53

densely packed resonance peaks in the measured FRFs pose significant challenges to system identification methods. Every effort was made to deal with this problem by carefully selecting *appropriate* range of the FRF. In Fig. 10 the ensemble mean calculated from the *identified* natural frequencies from *measured* frequency response functions, are compared with the Monte Carlo simulations. The experimentally identified values used in these plots are given in Table 2 for the purpose of possible comparisons using other analytical methods not considered in our paper. Like the beam experiment, the mean values obtained from the Monte Carlo simulation agree reasonably well with the experimental results for both methods. The standard deviation comparison in Fig. 11 show that the Monte Carlo estimates are lower than the measured values in the high- and low-frequency regimes, but not as much in the medium-frequency regime.

The normalized pdf plots shown in Figs. 12 and 13 compare the Monte Carlo simulation results with experimental data. The normalization is done according to Eq. (4). The agreement at the level of pdfs is satisfactory at high frequencies (eigenvalue number 30 in Fig. 12). The shift in the mean to the left of the origin for Monte Carlo simulation normalized pdfs is explained by Fig. 10. These results suggest that even when the first two moments can be predicted with reasonable accuracy using Monte Carlo simulations the higher moments may not agree. Although experimentally measured normalized pdfs are closer to Gaussian ensemble, albeit with nonzero mean, the Monte Carlo simulations are not.

These results also highlight an interesting aspect on how the choice of the FRF (that is the response point) can influence the pdf of the natural frequencies. The mean and standard deviation of the fifth natural frequency obtained using all three FRFs are quite similar. However, as can be seen from Figs. 12 and 13, the pdf of the fifth natural frequency obtained using the point 3 is significantly different from those obtained using the other two points. For the other three natural frequencies, however, the pdf obtained from all three points are fairly close. This shows the difficulty in comparing the pdf obtained using the Monte Carlo simulation and experiment. If response point 1 or 2 is selected, one might concluded that the Monte Carlo simulation results fit well with the experimental results. The same conclusion cannot be drawn when point 3 is selected.

V. Conclusions

The statistics of the eigenvalues of discrete linear dynamic systems with uncertainties have been considered using experimental methods on two structural systems of different modal densities. The first experiment is about a fixed–fixed beam with 12 randomly placed masses, and the second experiment is about a cantilever plate with 10 randomly placed oscillators. One hundred nominally identical beams and plates are created and individually tested using experimental modal analysis. Special measures have been taken so that the uncertainty in the natural frequencies only arises from the randomness in the mass and oscillator locations and the experiments are repeatable with minimum changes. Such novel measures include use of 1) a shaker as an impact hammer to ensure a consistent force and location for all of the tests, 2) a ruler to minimize the error in measuring the mass locations in the beam experiment, 3) a grid system and nodal points to minimize the error in measuring the oscillator and hammer locations in the plate experiment, 4) magnets as attached masses for the ease of placement in the beam experiment, and 5) magnets to attach the oscillators in the plate experiment.

Two methods (namely, the rational fraction polynomial method and a nonlinear least-squares technique) are used to extract the eigenvalues. These methods are applied to three FRFs for the beam experiment and six FRFs for the plate experiment. This implies that each of the two methods was applied to 300 FRFs for the beam experiment and 600 FRFs for the plate experiment. The following conclusions emerge from this study:

1) The ensemble statistics such as mean and standard deviation for natural frequencies vary with the spatial location of the measured FRFs and the type of the system identification technique chosen to estimate the natural frequencies.

2) Even when a reasonable prediction for the mean and sometimes for the standard deviations may be obtained using the Monte Carlo simulation, higher moments, and hence the pdfs can be significantly different.

3) In some cases, the differences in pdfs arising from different points and different identification methods can be more than those obtained from the Monte Carlo simulation.

It should be recalled that the above conclusions are based on a sample size of 100. Nevertheless, these results perhaps highlight the need for new outlook when one considers experimental works on random eigenvalue problems.

Acknowledgments

S. Adhikari gratefully acknowledges the support of the U.K. Engineering and Physical Sciences Research Council (EPSRC) through the award of an Advanced Research Fellowship and The Leverhulme Trust for the award of the Philip Leverhulme Prize. S. Phani thankfully acknowledges the financial support from the Natural Sciences and Engineering Research Council (NSERC), Canada through the Discovery Grant (371423-09) program.

References

[1] Shinozuka, M., and Yamazaki, F., "Stochastic Finite Element Analysis: An Introduction," *Stochastic Structural Dynamics: Progress in Theory and Applications*, edited by S. T. Ariaratnam, G. I. Schuëller, and I. Elishakoff, Elsevier Applied Science, London, 1998.

[2] Ghanem, R., and Spanos, P., *Stochastic Finite Elements: A Spectral Approach*, Springer–Verlag, New York, 1991.

[3] Kleiber, M., and Hien, T. D., *The Stochastic Finite Element Method*, Wiley, Chichester, England, U.K., 1992.

[4] Manohar, C. S., and Adhikari, S., "Dynamic Stiffness of Randomly Parametered Beams," *Probabilistic Engineering Mechanics*, Vol. 13, No. 1, Jan. 1998, pp. 39–51. doi:10.1016/S0266-8920(97)00006-4

[5] Manohar, C. S., and Adhikari, S., "Statistical Analysis of Vibration Energy Flow in Randomly Parametered Trusses," *Journal of Sound and Vibration*, Vol. 217, No. 1, 1998, pp. 43–74. doi:10.1006/jsvi.1998.1744

[6] Adhikari, S., and Manohar, C. S., "Dynamic Analysis of Framed Structures with Statistical Uncertainties," *International Journal for Numerical Methods in Engineering*, Vol. 44, No. 8, 1999, pp. 1157–1178. doi:10.1002/(SICI)1097-0207(19990320)44:8<1157::AID-NME549>3.0.CO;2-5

[7] Adhikari, S., and Manohar, C. S., "Transient Dynamics of Stochastically Parametered Beams," *Journal of Engineering Mechanics*, Vol. 126, No. 11, Nov. 2000, pp. 1131–1140. doi:10.1061/(ASCE)0733-9399(2000)126:11(1131)

[8] Haldar, A., and Mahadevan, S., *Reliability Assessment Using Stochastic Finite Element Analysis*, Wiley, New York, 2000.

[9] Boyce, W. E., "Random Eigenvalue Problems," *Probabilistic Methods in Applied Mathematics*, Academic Press, New York, 1968.

[10] Scheidt, J. V., and Purkert, W., *Random Eigenvalue Problems*, North Holland, New York, 1983.

[11] Ibrahim, R. A., "Structural Dynamics with Parameter Uncertainties," *Applied Mechanics Reviews*, Vol. 40, No. 3, 1987, pp. 309–328. doi:10.1115/1.3149532

[12] Benaroya, H., "Random Eigenvalues, Algebraic Methods and Structural Dynamic Models," *Applied Mathematics and Computation*, Vol. 52, No. 1, 1992, pp. 37–66. doi:10.1016/0096-3003(92)90097-K

[13] Manohar, C. S., and Ibrahim, R. A., "Progress in Structural Dynamics with Stochastic Parameter Variations: 1987 to 1998," *Applied Mechanics Reviews*, Vol. 52, No. 5, May 1999, pp. 177–197. doi:10.1115/1.3098933

[14] Manohar, C. S., and Gupta, S., "Modeling and Evaluation of Structural Reliability: Current Status and Future Directions," *Research Reviews in Structural Engineering*, edited by K. S. Jagadish, and R. N. Iyengar, Golden Jubilee, Bangalore, India, 2003.

[15] Kompella, M. S., and Bernhard, B. J., "Measurement of the Statistical Variations of Structural-Acoustics Characteristics of Automotive Vehicles," *SAE Noise and Vibration Conference* [CD-ROM], Society of Automotive Engineers, Warrendale, PA, 1993.

[16] Fahy, F., *Foundations of Engineering Acoustics*, Academic Press, London, 2000.

[17] Friswell, M. I., Coote, J. A., Terrell, M. J., Adhikari, S., Fonseca, J. R., and Lieven, N. A. J., "Experimental Data for Uncertainty Quantification," *Proceedings of the 23rd International Modal Analysis Conference (IMAC—XXIII)* [CD-ROM], Society of Experimental Mechanics (SEM), Orlando, FL, Feb. 2005.

[18] Shiryayev, O. V., Page, S. M., Pettit, C. L., and Slater, J. C., "Parameter Estimation and Investigation of a Bolted Joint Model," *Journal of Sound and Vibration*, Vol. 307, Nos. 3–5, Nov. 2007, pp. 680–697.
doi:10.1016/j.jsv.2007.06.033

[19] Ewins, D. J., *Modal Testing: Theory and Practice*, 2nd ed., Research Studies Press, Baldock, England, U.K., 2000.

[20] Collins, J. D., and Thomson, W. T., "The Eigenvalue Problem for Structural Systems with Statistical Properties," *AIAA Journal*, Vol. 7, No. 4, April 1969, pp. 642–648.
doi:10.2514/3.5180

[21] Hasselman, T. K., and Hart, G. C., "Modal Analysis of Random Structural System," *Journal of Engineering Mechanics*, Vol. 98, No. EM3, June 1972, pp. 561–579.

[22] Hart, G. C., "Eigenvalue Uncertainties in Stressed Structure," *Journal of Engineering Mechanics*, Vol. 99, No. EM3, June 1973, pp. 481–494.

[23] Ramu, S. A., and Ganesan, R., "Stability Analysis of a Stochastic Column Subjected to Stochastically Distributed Loadings Using the Finite Element Method," *Finite Elements in Analysis and Design*, Vol. 11, No. 2, 1992, pp. 105–115.
doi:10.1016/0168-874X(92)90045-E

[24] Ramu, S. A., and Ganesan, R., "Stability of Stochastic Leipholz Column with Stochastic Loading," *Archive of Applied Mechanics*, Vol. 62, 1992, pp. 363–375.
doi:10.1007/BF00804597

[25] Ramu, S. A., and Ganesan, R., "A Galerkin Finite Element Technique for Stochastic Field Problems," *Computer Methods in Applied Mechanics and Engineering*, Vol. 105, No. 3, 1993, pp. 315–331.
doi:10.1016/0045-7825(93)90061-2

[26] Ramu, S. A., and Ganesan, R., "Parametric Instability of Stochastic Columns," *International Journal of Solids and Structures*, Vol. 30, No. 10, 1993, pp. 1339–1354.
doi:10.1016/0020-7683(93)90216-T

[27] Sankar, T. S., Ramu, S. A., and Ganesan, R., "Stochastic Finite Element Analysis for High Speed Rotors," *Journal of Vibration and Acoustics*, Vol. 115, No. 1, 1993, pp. 59–64.
doi:10.1115/1.2930315

[28] Song, D., Chen, S., and Qiu, Z., "Stochastic Sensitivity Analysis of Eigenvalues and Eigenvectors," *Computers and Structures*, Vol. 54, No. 5, 1995, pp. 891–896.
doi:10.1016/0045-7949(94)00386-H

[29] den Nieuwenhof, B. V., and Coyette, J.-P., "Modal Approaches for the Stochastic Finite Element Analysis of Structures with Material and Geometric Uncertainties," *Computer Methods in Applied Mechanics and Engineering*, Vol. 192, Nos. 33–34, 2003, pp. 3705–3729.
doi:10.1016/S0045-7825(03)00371-2

[30] Grigoriu, M., "A Solution of Random Eigenvalue Problem by Crossing Theory," *Journal of Sound and Vibration*, Vol. 158, No. 1, 1992, pp. 69–80.
doi:10.1016/0022-460X(92)90664-J

[31] Lee, C., and Singh, R., "Analysis of Discrete Vibratory Systems with Parameter Uncertainties, Part I: Eigensolution," *Journal of Sound and Vibration*, Vol. 174, No. 3, 1994, pp. 379–394.
doi:10.1006/jsvi.1994.1282

[32] Nair, P. B., and Keane, A. J., "An Approximate Solution Scheme for the Algebraic Random Eigenvalue Problem," *Journal of Sound and Vibration*, Vol. 260, No. 1, 2003, pp. 45–65.
doi:10.1016/S0022-460X(02)00899-4

[33] Hála, M., "Method of Ritz for Random Eigenvalue Problems," *Kybernetika*, Vol. 30, No. 3, 1994, pp. 263–269.

[34] Mehlhose, S., von Scheidt, J., and Wunderlich, R., "Random Eigenvalue Problems for Bending Vibrations of Beams," *Zeitschrift fur Angewandte Mathematik und Mechanik*, Vol. 79, No. 10, 1999, pp. 693–702.
doi:10.1002/(SICI)1521-4001(199910)79:10<693::AID-ZAMM693>3.0.CO;2-0

[35] Szekely, G. S., and Schuëller, G. I., "Computational Procedure for a Fast Calculation of Eigenvectors and Eigenvalues of Structures with Random Properties," *Computer Methods in Applied Mechanics and Engineering*, Vol. 191, Nos. 8–10, 2001, pp. 799–816.
doi:10.1016/S0045-7825(01)00290-0

[36] Pradlwarter, H. J., Schuëller, G. I., and Szekely, G. S., "Random Eigenvalue Problems for Large Systems," *Computers and Structures*, Vol. 80, Nos. 27–30, 2002, pp. 2415–2424.
doi:10.1016/S0045-7949(02)00237-7

[37] Du, S., Ellingwood, B. R., and Cox, J. V., "Initialization Strategies in Simulation-Based SFE Eigenvalue Analysis," *Computer-Aided Civil and Infrastructure Engineering*, Vol. 20, No. 5, 2005, pp. 304–315.
doi:10.1111/j.1467-8667.2005.00398.x

[38] Ghosh, D., Ghanem, R. G., and Red-Horse, J., "Analysis of Eigenvalues and Modal Interaction of Stochastic Systems," *AIAA Journal*, Vol. 43, No. 10, 2005, pp. 2196–2201.
doi:10.2514/1.8786

[39] Adhikari, S., "Complex Modes in Stochastic Systems," *Advances in Vibration Engineering*, Vol. 3, No. 1, 2004, pp. 1–11.

[40] Verhoosel, C. V., Gutiérrez, M. A., and Hulshoff, S. J., "Iterative Solution of the Random Eigenvalue Problem with Application to Spectral Stochastic Finite Element Systems," *International Journal for Numerical Methods in Engineering*, Vol. 68, No. 4, 2006, pp. 401–424.
doi:10.1002/nme.1712

[41] Rahman, S., "A Solution Of The Random Eigenvalue Problem by a Dimensional Decomposition Method," *International Journal for Numerical Methods in Engineering*, Vol. 67, No. 9, 2006, pp. 1318–1340.
doi:10.1002/nme.1665

[42] Adhikari, S., "Random Eigenvalue Problems Revisited," *Sadhana. Academy Proceedings in Engineering Sciences*, Vol. 31, No. 4, Aug. 2006, pp. 293–314.
doi:10.1007/BF02716778

[43] Adhikari, S., "Joint Statistics of Natural Frequencies of Stochastic Dynamic Systems," *Computational Mechanics*, Vol. 40, No. 4, Sept. 2007, pp. 739–752.
doi:10.1007/s00466-006-0136-8

[44] Adhikari, S., and Friswell, M. I., "Random Matrix Eigenvalue Problems in Structural Dynamics," *International Journal for Numerical Methods in Engineering*, Vol. 69, No. 3, 2007, pp. 562–591.
doi:10.1002/nme.1781

[45] Mehta, M. L., *Random Matrices*, 2nd ed., Academic Press, San Diego, CA, 1991.

[46] Muirhead, R. J., *Aspects of Multivariate Statistical Theory*, Wiley, New York, 1982.

[47] Edelman, A., "Eigenvalues and Condition Numbers of Random Matrices," *SIAM Journal on Matrix Analysis and Applications*, Vol. 9, No. 4, 1988, pp. 543–560.
doi:10.1137/0609045

[48] Dumitriu, I., and Edelman, A., "Matrix Models for Beta Ensembles," *Journal of Mathematical Physics*, Vol. 43, No. 11, 2002, pp. 5830–5847.
doi:10.1063/1.1507823

[49] Adhikari, S., Friswell, M. I., Lonkar, K., and Sarkar, A., "Experimental Case Studies for Uncertainty Quantification in Structural Dynamics," *Probabilistic Engineering Mechanics*, Vol. 24, No. 4, Oct. 2009, pp. 473–492.
doi:10.1016/j.probengmech.2009.01.005

[50] Maia, N. M. M., and Silva, J. M. M. (ed.), *Theoretical and Experimental Modal Analysis*, Engineering Dynamics Series, Research Studies Press, Taunton, England, U.K., 1997.

[51] Silva, J. M. M., and Maia, N. M. M. (eds.), *Modal Analysis and Testing: Proceedings of the NATO Advanced Study Institute* [CD-ROM], NATO Science Series: E: Applied Science, 3–15 May 1998.

[52] Adhikari, S., "Modal Analysis of Linear Asymmetric Non-Conservative Systems," *Journal of Engineering Mechanics*, Vol. 125, No. 12, Dec. 1999, pp. 1372–1379.
doi:10.1061/(ASCE)0733-9399(1999)125:12(1372)

[53] Adhikari, S., "Lancaster'S Method of Damping Identification Revisited," *Journal of Vibration and Acoustics*, Vol. 124, No. 4, Oct. 2002, pp. 617–627.
doi:10.1115/1.1500742

[54] Adhikari, S., "Optimal Complex Modes and an Index of Damping Non-Proportionality," *Mechanical Systems and Signal Processing*, Vol. 18, No. 1, Jan. 2004, pp. 1–27.
doi:10.1016/S0888-3270(03)00048-7

[55] Press, W. H., Teukolsky, S. A., Vetterling, W. T., and Flannery, B. P., *Numerical Recipes in C*, Cambridge Univ. Press, Cambridge, England, U.K., 1992.

[56] Duffour, P., *Modal Testing on Violin Bodies*, Cambridge Univ., Engineering Dept., Cambridge, England, U.K., 1998.

[57] Goyal, V. K., and Kapania, R. K., "Dynamic Stability of Uncertain Laminated Beams Subjected to Subtangential Loads," *International Journal of Solids and Structures*, Vol. 45, No. 10, 2008, pp. 2799–2817.
doi:10.1016/j.ijsolstr.2007.11.024

[58] Adhikari, S., and Sarkar, A., "Uncertainty in Structural Dynamics: Experimental Validation of Wishart Random Matrix Model," *Journal of Sound and Vibration*, Vol. 323, Nos. 3–5, 2009, pp. 802–825.
doi:10.1016/j.jsv.2009.01.030

[59] Dawe, D., *Matrix and Finite Element Displacement Analysis of Structures*, Oxford Univ. Press, Oxford, 1984.

R. Kapania
Associate Editor